Korean J. Chem. Eng., 40(8), 1863-1870 (2023)
DOI: 10.1007/s11814-023-1490-3

pISSN: 0256-1115
eISSN: 1975-7220

Investigation of heat transfer of the frame of entrance door encompassing phase change materials through computational fluid dynamics schemes

Alireza Arab Solghar*, Seyed Hossein Ahsaei*, Afshin Iranmanesh, and Mohammad Shafiey Dehaj*,†**

*Department of Mechanical Engineering, Faculty of Engineering, Vali-e-Asr University of Rafsanjan, Iran
**Department of Civil Engineering, Faculty of Engineering, Vali-e-Asr University of Rafsanjan, Iran
(*Received 16 December 2022 • Revised 1 May 2023 • Accepted 3 May 2023*)

Abstract−Embedment of phase change materials (PCMs) in buildings elements is a technique to lower the heating and cooling demands. In the present study, a frame of entrance doors filled with the PCMs was simulated for a sunny summer day condition of Rafsanjan city in Iran. It was assumed that the frame is subjected to the indoor and outdoor temperature and solar radiation. The simulation was carried out through 2-D finite element method taking into account heat and mass transfer in the PCM. A parametric study was conducted to investigate the type of PCMs, the volume PCMs as well as their positions in the frame. The results were compared with a common frame filled with air. The obtained findings showed that RT-25 is more effective than capric acid, paraffin and P116. Maximum reduction of heat flux was observed to be 37.72% for the frame filled with RT-25 when its outside walls were in contact with the PCM. The results also reveal that the incorporation of the PCM is effective for passive thermal storage.

Keywords: Phase Change Materials, Solar Radiation, Frame, Passive Solar Heat Storage

INTRODUCTION

Global warming is one of the most important issues in the current century. Buildings are responsible for 40% of global final energy consumption and the emissions of greenhouse gases [1]. Therefore, it is necessary to develop technologies for the reduction of energy consumption in the building and consequent pollutant emissions. The embedment of phase change materials (PCMs) into building components, such as side walls, ceilings and floors, has been studied as an alternative technique for passive solar thermal storage. The PCMs can decrease the energy consumption of the buildings via two main ways: (1) Owing to the high latent heat of the PCMs at a specified temperature, they behave similar to an isothermal energy reservoir which can absorb and release a quantity of heat without any change in their temperature; (2) Due to the thermal storage properties of the PCMs, the heating and cooling load of the indoor space can be shifted and decreased.

In the literature, there are some reviews considering the embedment of the PCMs into the building elements [2-5]. In fact, organic, inorganic and eutectic PCMs are three main kinds of PCMs which are suitable for building cooling or heating because of the technical limitation of other varieties. The selection of the PCM is limited by the region's climate [6]. Also, thermophysical properties of the PCMs, such as melting temperature, latent heat, thermal capacity and thermal conductivity, are rather significant for reliability of efficient incorporation in the buildings elements [7-10]. Furthermore, Alam et al. [11] determined that the performance of the PCM depends on the type, quantity and position of the PCM in the building components as well as the region climate. Cabeza et al. [12] showed that the embedment of a microencapsulated PCM in a concrete wall leads to higher heat storage, enhanced thermal inertia performance and lower fluctuation of the indoor temperature compared with common concrete walls.

In a numerical investigation, Jin et al. [13] concluded that the optimal location of the PCM layer depends on the PCM thermal properties and local conditions. They found that as the thickness layer, latent heat and melting temperature of the PCM increase, the PCM should be closer to the exterior surface of the wall. Also, Xie et al. [14] reported the PCM thermal efficiency is a function of the month and specified the months that the PCM effect is considerable.

Thermal characteristics of the PCMs accompanied with thermal insulation have been studied extensively. Through a simplified model, Halford and Boehm [15] deduced that a layer of PCM surrounded by two layers of fiberglass layers decreases the heat load up to 57%. Fateh et al. [16] carried out a numerical study and determined that incorporation of the PCMs at a different position into a light weight wall accompanied with a layer of insulation is effective in the reduction of heat transfer. For some cities of Iran, Baniassadi et al. [17] conducted an economic analysis and found that the thermal insulation is more economical than the use of PCM. Furthermore, Ye et al. [22] compared the thermal performance of the PCM and thermal insulation. They showed that for the cold season, the PCM is more efficient while the thermal insulation is more effective under the yearly energy consumption.

To investigate the thermal performance of brick with PCMs, Alawadhi [18] numerically examined the thermal performance of a brick containing the PCM capsule. It was reported that the rate of heat transfer decreases by the insertion of the PCM and the increase of the PCM volume. It was also concluded that heat transfer is

†To whom correspondence should be addressed.
E-mail: m.shafiey@vru.ac.ir

minimum when the PCM is embedded in the centerline of the brick. Additionally, Izquierdo-Barrientos et al. [19] investigated the effect of PCMs in the exterior walls of the buildings. They employed a 1-D unsteady model to study the heat transfer rate. They conducted a parametric investigation regarding the effect of the PCM location and orientation, outdoor conditions and melting temperature of the PCM. Their findings show that by appropriate selection of the PCMs with respect to the season and wall positioning, the amplitude of the heat transfer decreases. They reported that the reduction of heat transfer is insignificant irrespective of the PCM melting temperature and wall positioning. Also, Wang et al. [20] investigated the impact of the PCM layer thickness and position in the wall on the reduction of heat transfer rate. They deduced that the maximum reduction of heat transfer is 34.9% for a 20 mm RT42 layer exposed to the outdoor conditions.

To find the influence of the PCMs' physical properties on the heat loss from the buildings, Kant et al. [21] studied the effect of PCMs types on the reduction of heat transfer in the brick in which its cavities were filled with the PCMs. They found that capric acid is more efficient than paraffin and RT-25 for the considered problem. Also, it was concluded that the volume of the PCMs is an influential parameter for the control of the heat transfer rate.

In a numerical work, Saafi and Daouas [22] carried out energy and economic analysis of using the PCMs integrated with the brick. The results show that the incorporation of the PCM in the wall brick is cost-ineffective for a period of 30 years. The PCM displayed better efficiency in the absence of thermal insulation. They also showed that when the PCM is inserted on the external surface of the brick, the energy efficiency improves. It was determined that by addition of the PCM, the time lag is shifted for 2 hours due to the enhancement of thermal inertia of the wall.

Moreover, Arıcı et al. [23] numerically examined the influence of latent heat of PCM on the thermal mass of the wall. They also optimized the thickness of PCM layer to lower buildings energy consumption. They assumed two configurations of the wall, which the location of PCM varied from adjacent to the interior plaster to adjacent to the exterior plaster. The computations were carried out under three different climate conditions in Turkey. Moreover, Arıcı et al. used two layers of PCM rather than one to increase the thermal energy storage of PCM to minimize thermal loads. They found that two PCM layers, one on the outside side of the wall and the other on the interior side, yielded a higher annual energy savings versus a single layer of PCM [24].

To improve the low thermal conductivity of PCMs, which limits their potential benefits, Tuncbilek et al. [25] suggested adding metal nanoparticles with high thermal conductivity to PCMs. They found that the nanoparticle addition decreased the energy-saving performance of PCM since the reduction in the thermal resistance and latent heat capacity caused by the nanoparticles loading was more profound than the augmentation obtained by the enhancement of latent heat exploitation caused by the increased thermal conductivity.

In most parts of Iran during summer season, consumption of electrical energy to run the equipment of air conditioning systems surges up drastically year by year. Also, the rate of heat transfer to the indoor space is a great function of solar radiation on the exterior walls, windows and opening doors. Thus, it is vital to lower the heat transfer rate to the indoor space. The decline of energy consumption and enhancement of energy storage of the buildings are rather important for the rise of energy effectiveness. Moreover, decreasing the electricity demand of the air conditioning devices is crucial for the constancy of electricity network. There are several studies focusing on the employment of the PCMs into the walls [26-29] and the roofs [30-32]. These all have motivated the present work dealing with the decrease of heat transfer rate to the buildings through employment of the PCMs in the frame of the entrance doors under the environmental conditions of Rafsanjan city and construction code of Iran. The frames of external doors and windows subjected to the solar radiation act like a thermal bridge which dramatically affects the energy consumption of the building [33]. Increasing thermal inertia of these frames and investigating the effect of the PCM insertion in the frames are the main goal of the present study. Therefore, influential parameters such as the type of PCMs, location of embedded PCM and quantity of the PCMs have been extensively investigated.

PROBLEM DESCRIPTION

In the current study, a frame of inlet door of the buildings was considered to investigate the influence of the PCMs on the heat lag

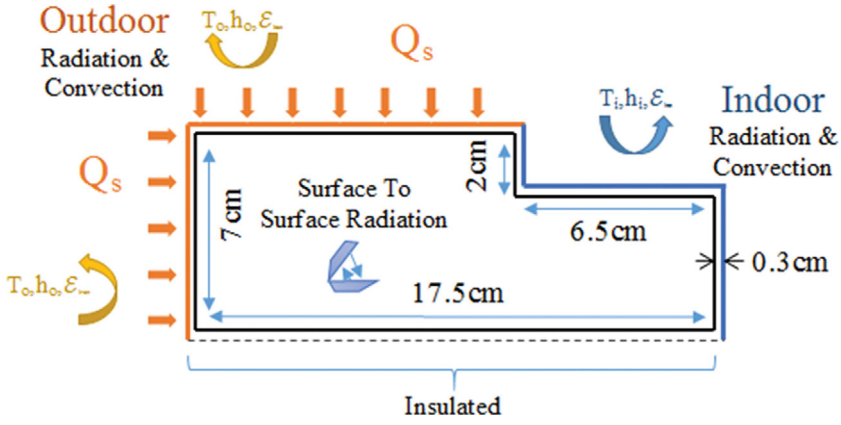

Fig. 1. Outline of the frame with boundary conditions.

and reduction to the indoor space. In Fig. 1, the geometrical configuration of the studied case with the boundary conditions is displayed. Two sides of the frame are exposed to the outdoor space, while the two other sides of the frame are exposed to the indoor space. It is assumed that the open-air sides of the frame are subjected to solar radiation and convective heat transfer. Also, the inner sides of the frame are subjected to convection heat transfer as well as radiative heat loss to the environment. The convection heat transfer coefficient is set at 10 W/(m^2·K) and 20 W/(m^2·K) for the inner and outer surface, respectively [18]. Moreover, surface to surface radiation and natural convection are considered inside the frame. The bottom side of the frame is assumed to be insulated as depicted in Fig. 1. The initial temperature of the entire frame is assumed to be at 25 °C. Four different types of PCMs, namely, Paraffin, P116, Capric acid and RT-25, in a plastic container with the thickness of 3 mm are taken into account for the present work. In Fig. 2, the variations of air temperature and solar radiation of Rafsanjan-Iran are presented for 15 July 2017. The physical properties of the frame, plastic container and PCMs are summarized in Table 1.

In fact, the heat transfer in the frame is three dimensional; nevertheless, the height of the frame is too large compared to its width, and thus the end effect of the frame has a negligible impact on the rate of heat transfer in the frame.

The properties of the frame are considered to be temperature independent, while for the PCMs, the thermo-physical properties depend on the temperature. Note that for sake of simplicity the thermal expansion of the PCMs and frame is assumed to be negligible. In the current work, the heat transfer in the frame of the entrance door encompassing the PCMs in an enclosure was investigated.

For the sides of the frame being exposed to the solar radiation and ambient conditions, the conservation equation of energy is given from the following relation:

$$-k_{fr}\nabla T_{fr}=h_o(T_o-T_{fr})+\varepsilon_{fr}\sigma(T_o^4-T_{fr}^4)+\alpha_{fr}E(t) \quad (1)$$

where k_{fr} is the thermal conductivity of the frame, T_{fr} is the frame temperature, h_o is the convection heat transfer coefficient of the outdoor environment, T_o is the outdoor environment temperature, σ is the Stefan-Boltzmann constant, ε_{fr} is the emissivity of the frame, α_{fr} is the absorptivity coefficient and E is the rate of incident solar radiation.

Also, the heat transfer of the frame to the indoor space can be written as the following:

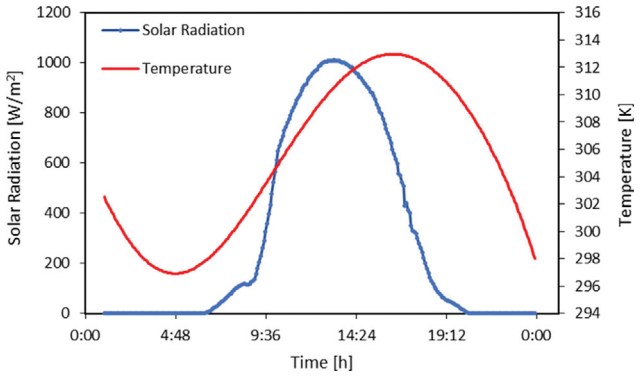

Fig. 2. Ambient temperature and solar radiation variation for 15 July in Rafsanjan, Iran.

$$-k_{fr}\nabla T_{fr}=h_i(T_i-T_{fr})+\varepsilon_{fr}\sigma(T_i^4-T_{fr}^4) \quad (2)$$

where h_i is the convection heat transfer coefficient of the indoor environment and T_i is the indoor temperature.

Inside the frame, the heat transfer occurs via the natural convection and radiation that can be written as:

$$\rho C_p\frac{\partial T_{fr}}{\partial t}+\rho C_p V\nabla T_{fr}=k\nabla^2 T-\frac{1}{\rho C_p}\nabla\cdot\vec{q}_r \quad (3)$$

where V is the velocity field of the air inside the frame and q_r is the radiative flux vector. The flow field of the air is obtained from simultaneous solution of the conservation of mass, momentum and energy equations. Therefore, respectively, the mass and momentum equations of a transient, incompressible and laminar flow of the air neglecting the viscous dissipation are expressed as:

$$\nabla\cdot\vec{V}=0 \quad (4)$$

$$\frac{\partial\vec{V}}{\partial t}+\vec{V}\cdot\nabla\vec{V}=-\frac{1}{\rho}\nabla p+\nabla^2\vec{V} \quad (5)$$

where p is the air pressure. The divergence of radiative heat flux in Eq. (3) is given as follows:

$$\nabla\cdot\vec{q}=\kappa_a\left(4\pi I_b(\vec{r})-\int_{4\pi} I(\vec{r},\vec{s})d\Omega\right) \quad (6)$$

where, κ_a is the absorption coefficient, I is the radiation intensity and I_b is the black body radiation intensity. To compute the diver-

Table 1. Thermophysical properties of the studied materials

Material		RT-25	Paraffin [*]	Capric acid	P116	Iron [20]	Acrylic plastic [20]	Air [20]
Melting temperature (C)		26.6	28.2	32.0	47.0	NA	NA	NA
Latent heat (kJ/kg)		232	245	152.7	225	NA	NA	NA
Thermal conductivity (W/(mK))	s	0.19	0.35	0.37	0.24	76.2	0.18	0.024
	l	0.18	0.15	0.15	0.24			
Density (kg/m^3)	s	785	814	1,018	830	7,870	1,190	1.125
	l	749	775	888	773			
Specific Heat (kJ/(kgK))	s	1.8	1.9	1.9	2.4	0.44	17.4	1.01
	l	2.4	2.2	2.4	1.9			

l (liquid), s (solid), NA (Not Applicable), * obtained from COMSOL library

gence of radiative heat flux in the air, the radiative transfer equation (RTE) should be solved, so for an absorbing, emitting and scattering gray medium the RTE is given through the following equation [34]:

$$(\vec{s}\cdot\nabla)I(\vec{r},\vec{s}) = \beta_r\left\{-I(\vec{r},\vec{s})+(1-\omega)I_b(\vec{r})+\frac{\omega}{4\pi}\int_{4\pi} I(\vec{r},\vec{s})\varphi(\vec{s}'\rightarrow\vec{s})d\Omega'\right\} \quad (7)$$

in which β is the extinction coefficient, ϕ is the scattering phase function and $d\Omega$ is the solid angle. The boundary condition for a diffusely emitting and reflecting gray of the frame's wall is expressed as follows:

$$I(\vec{r}_w,\vec{s}) = \varepsilon_w I_b(\vec{r}_w)+\frac{(1-\varepsilon_w)}{\pi}\int_{n_w\cdot\vec{s}'<0} I(\vec{r}_w,\vec{s})|\vec{n}_w\cdot\vec{s}|d\Omega',\ n_w\cdot\vec{s}'>0 \quad (8)$$

where ε_w is the emissivity of the frame's wall.

The temperature dependent properties of the PCMs are obtained from the following relations:

$$\rho_{PCM}(T)=\rho_s+B(T)(\rho_l-\rho_s) \quad (9)$$

$$k_{PCM}(T)=k_s+B(T)(k_l-k_s) \quad (10)$$

$$C_{P,PCM}(T)=C_{P,s}+B(T)(C_{P,l}-C_{P,s})+\lambda D(T) \quad (11)$$

in which λ is latent heat of the PCMs. B(T) and D(T) are expressed as follows, respectively:

$$B(T)=\begin{cases}0 & T<T_s\\ \dfrac{T-T_s}{T_l-T_s} & T_s\le T\le T_l\\ 1 & T>T_l\end{cases} \quad (12)$$

$$D(T)=\exp\left(\frac{-(T-T_s)^2}{(T_l-T_s)^2}/\sqrt{\pi(T_l-T_s)^2}\right) \quad (13)$$

where T_s and T_l are the solidification temperature and the melting temperature, respectively. Note that B(T) of the PCMs is equal to zero for the solid phase and is equal to 1 for the liquid phase. Besides, B(T) varies linearly under the transition condition [21]. Also, the value of D(T) is always equal to zero except in the transition zone.

RESULTS AND DISCUSSION

The conservation of mass, momentum and energy equations governing the problem were numerically solved through COMSOL Multi-physics 5.4 software employing the finite element method (FEM). Also the required initial and boundary conditions and the physical properties of the geometry and the PCM were implemented in the software. The geometry of the door framework was appropriately created in the software. Regular rectangular meshing was used for the problem as depicted in Fig. 3. Moreover, the mesh study was carried out for the present study which 19108 elements were selected for the problem solution with the size of 0.75 mm for each element, and also the time step was obtained to be 5 second.

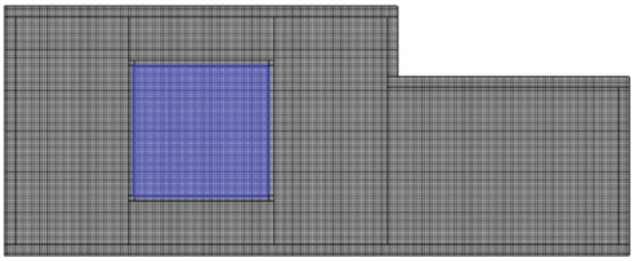

Fig. 3. Mesh generation of the body and the PCM.

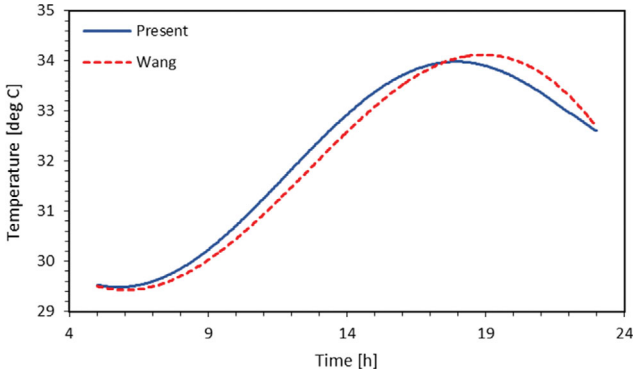

Fig. 4. Comparison between the present result and findings of Wang et al. [20].

To validate the present employed model, the results were compared against the study of Wang et al. [20] as displayed in Fig. 4. As seen, the present results are in acceptable agreement with those of Wang et al. [20]. It is noted that for the sake of accuracy the thermophysical properties of the PCMs are considered temperature dependent.

In this study, the presence of four different types of PCMs inside the body was investigated to characterize the thermal behavior of the body under different locations and masses of the PCMs. The PCMs were assumed to be capric Acid, paraffin, P116 and RT-25.

The computations were carried out for 15 June through meteorological data of Rafsanjan city in Iran.

To analyze the effect of the PCM location inside the geometry, three possible configurations were considered as illustrated in Fig. 5. Fig. 6 depicts the variation of the heat flux entering the space through the body as a function of the PCM location for paraffin compared with the case that the body is thoroughly filled with air

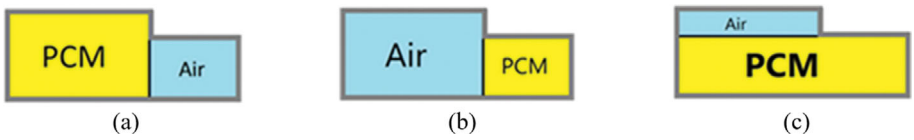

Fig. 5. Different configurations of the body loaded with the PCM: (a) position 1, (b) position 2, (c) position 3.

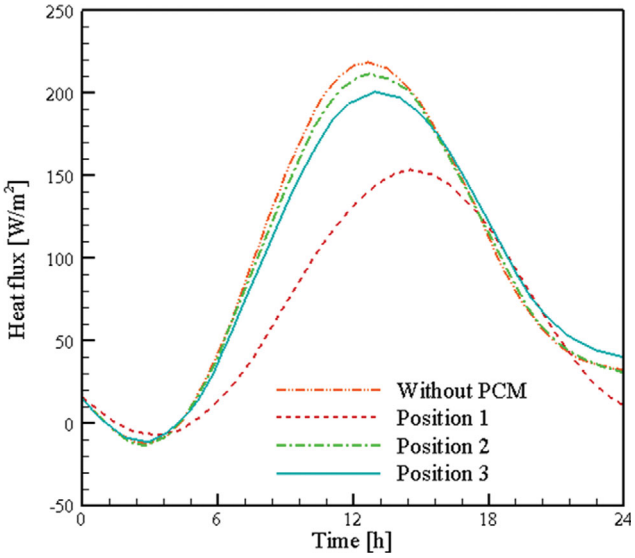

Fig. 6. Variation of the heat flux through the body as a function of the PCM position.

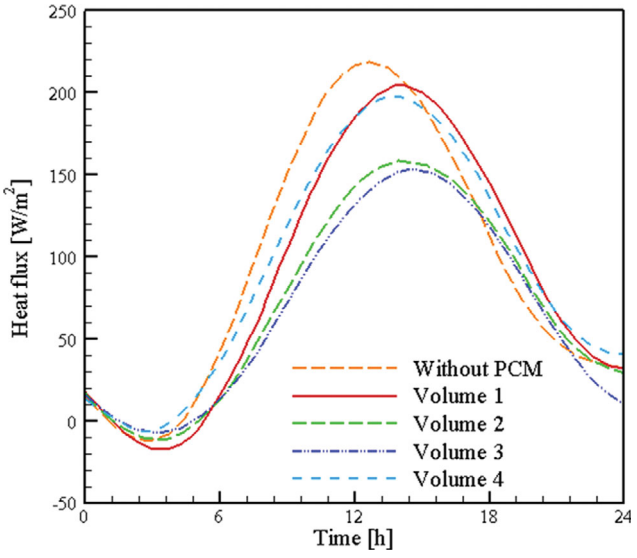

Fig. 9. Variation of heat flux vs. time for different volume of the PCM inside the frame.

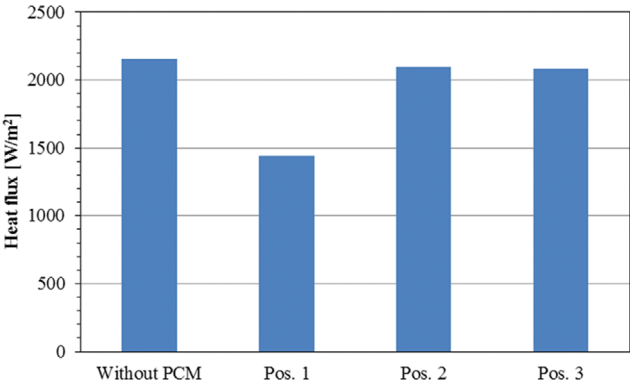

Fig. 7. Total heat flux to the indoor space as a function of the PCM position.

(without any PCM). As seen, the first configuration gives the minimum heat flux among the other studied arrangements in which the heat flux is lowered by 33.1% compared to the body without any PCM. In the second arrangement, the reduction of heat flux is 2.9% compared to the body filled with air. Moreover, in the third configuration, heat flux decreases by 3.5% compared with air filled case. This reduction among the configurations shows the influence of the presence of the PCM inside the geometry. The comparison of the results displayed in Fig. 6 reveals that as the mass of the PCM decreases, the presence of the PCM is less effective in the reduction of the heat flux. Accordingly, Fig. 7 shows the total heat flux in the day by integrating the heat flux over the time. It is clear that the difference between the total heat flux of the air filled body (maximum amount of heat loss among considered cases) and the body with the PCM in the first configuration is 720 W/m^2. The figure demonstrates that the presence of a PCM and its volume has a substantial effect on the reduction of the heat flux.

The effect of the PCMs' volume on the heat transfer rate to the indoor space is further examined via Fig. 8 and 9. According to Fig. 8, the volume of the PCM was considered for four different values. From the results shown in Fig. 9, the volume of the PCM has significant effect on the rate of heat transfer to the indoor space, such that for the cases displayed in Fig. 8(a) and (b), it is clear that the heat transfer rate to the indoor space decreases considerably compared with the case without any PCM at all hours of the day. While for the configuration (c) and (d) of Fig. 8, the rate of heat transfer is not always less than the air-filled case. For better comparison, the total heat flux is illustrated in Fig. 10. Against the expectation, it can be seen that when the profile is completely filled with the PCM, the rate of heat transfer does not considerably decrease compared with the air-filled case. This is because when the PCM receives the heat flux from the outdoor source, it melts down and then it becomes a liquid, which since then the heat transfers via conduction to the indoor space. Therefore, filling the body with the PCM should be accurately and cautiously carried out. It is clear that the presence of air inside the body is too important on the controlling the rate of heat transfer, because the heat transfers via the all heat transfer mechanisms, i.e., conduction, convection and radia-

Fig. 8. Different PCM volume inside the frame; (a) volume 1, (b) volume 2, (c) volume 3, (d) volume 4.

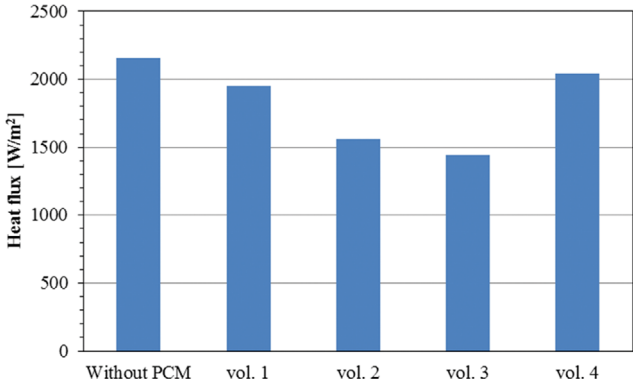

Fig. 10. Total heat flux to the indoor space for different volume of the PCM inserted into the frame.

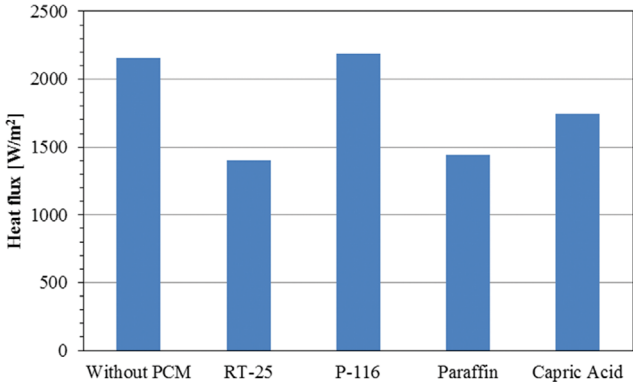

Fig. 12. Total heat flux to the indoor space vs. different types of the PCMs.

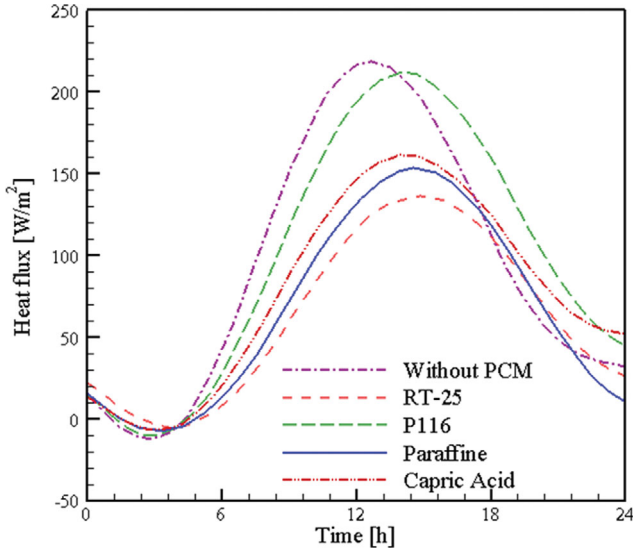

Fig. 11. Effect of the PCMs type on the rate of heat transfer.

tion, while for the PCMs, the transfer of heat occurs through two process, first, liquefaction (when receive thermal heat) or solidification (when lose thermal heat) it means change of the phase, then the conduction heat transfer becomes dominant.

To study the influence of the PCMs' type on the rate of heat transfer to the indoor space being compared with the air-filled frame, four different PCMs were considered in the computations: capric acid, paraffin, P116 and RT-25. Therefore, the results were obtained and compared for the configuration of Fig. 5(a). In Fig. 11, the heat flux to the indoor space is depicted during the studied day. As seen, the largest reduction of the heat transfer rate to the indoor space is for RT-25, which the decrease is 35% compared with the air-filled case (Fig. 12). Also, the peak point of the heat flux to the indoor space is different for all the considered cases, such that the highest heat lag occurs for RT-25.

To have a good insight about the total heat transfer rate to the indoor space for the day, the results were summarized in Tables 2 and 3. Tables 2 and 3 show the total heat flux along X and Y- axis for all considered cases of Fig. 8 and all types of the considered PCMs, respectively. Note that the use of P-116 has inverse impact on the rate of heat transfer in which the total heat transfer rate increases with respect to the air-filled case. This might be due to the high melting temperature of P-116, which its change of the phases is insignificant in the day. As seen from the table, RT-25 yields the best results considering the reduction of heat flux to the indoor space.

Table 2. The reduction percent of the heat flux along X-axis for the geometries of Fig. 8

PCM	Volume (a)	Volume (b)	Volume (c)	Volume (d)
Capric acid	5.36	15.78	19.04	2.89
Paraffin	9.60	27.74	33.36	5.19
RT-25	10.09	22.19	35.16	5.39
P 116	−0.33	−1.12	−1.47	−0.20

Table 3. The reduction percent of the heat flux along Y-axis for the geometries of Fig. 8

PCM	Volume (a)	Volume (b)	Volume (c)	Volume (d)
Capric acid	5.47	16.14	19.82	0.67
Paraffin	10.10	29.84	35.13	1.30
RT-25	10.54	31.18	37.72	9.11
P 116	−0.59	−1.86	−2.25	−0.55

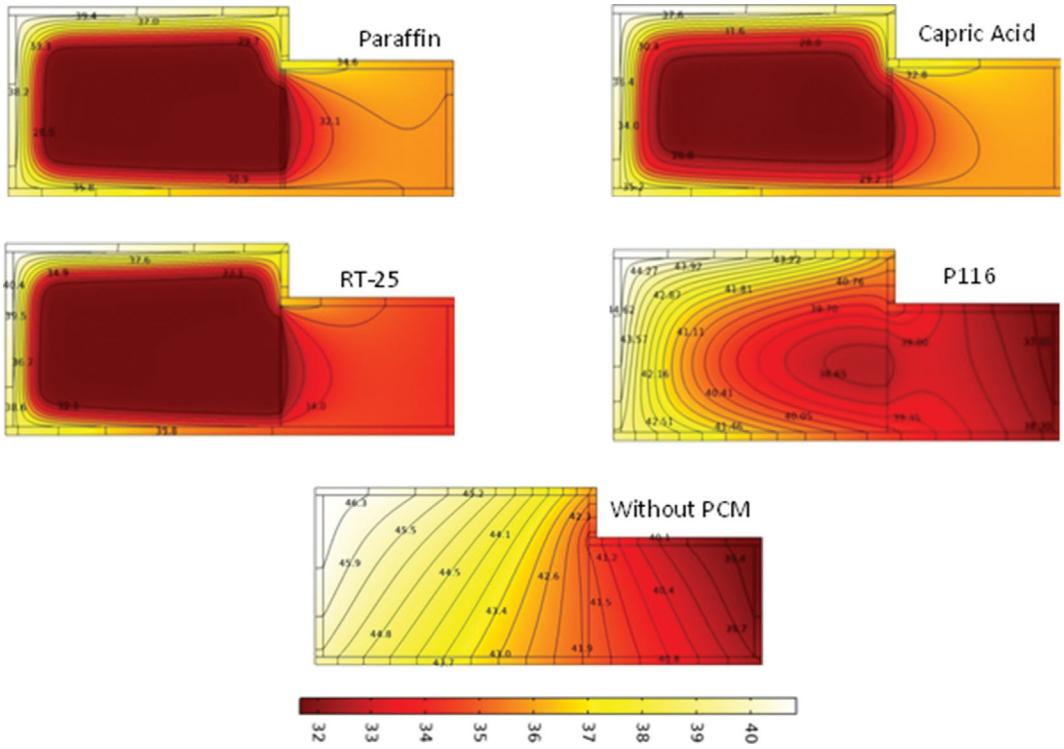

Fig. 13. The isotherms distribution of the frame at 12 AM for different PCMs and without PCM.

Fig. 13 displays the isothermal lines inside the frame at 12 AM for different types of the considered PCMs and without PCM for the configuration of Fig. 5(a). It is noted that in the daytime, the PCMs absorbs the thermal heat from the source till they melt down; the absorbed heat till the melting down is latent heat which is released during the night time. So, the energy that is absorbed by the PCM via its latent heat decreases the heat transfer to the indoor space. As seen from Fig. 13, the isotherms are distorted near the paraffin, capric acid and RT-25, while they are parallel to the vertical wall of the frame for P116, indicating that for P116, the change of phase has not completely occurred and it acts as a semi-solid substance, which the heat transfers via conduction during the day. Moreover, for the case without PCM, the isotherms are parallel to the walls, indicating high temperature gradient, which leads to higher rate of the heat transfer.

CONCLUSIONS

A numerical study was carried out to investigate the effectiveness of the PCM embedded in a specific kind of frame of entrance doors. Time dependent outdoor ambient temperature was considered in the computations according to the hottest day of Rafsanjan-Iran in 2017. The reduction of the heat transfer rate was considered as a criterion for the effectiveness of the PCMs. Therefore, the effect of the PCM type, volume and position on the reduction of heat flux through the frame was explored varying with the time. The results showed that maximum reductions of heat are 19.82%, 35.13% and 37.72% for capric acid, parrafin and RT-25, respectively. It was also found that P116 has no impact on the reduction of heat transfer. Also, the position and the volume of the PCMs are significant parameters for the studied cases. The results display that the PCM in throughout contact with those walls of frame which are subjected to the outdoor conditions yields the best performance.

An economic optimization study can be carried out to find the optimum value of PCM as a function of the initial cost, saved energy and its corresponding payback time.

NOMENCLATURE

C_p : specific heat [J/(kg·K)]
E : incident solar radiation [W/m^2]
I : radiation intensity [W/m^2]
I_b : black body radiation intensity [W/m^2]
h : heat transfer coefficient [W/(m^2 K)]
k : thermal conductivity [W/(mK)]
P : pressure [Pa]
T : temperature [°C]
t : time [s]
T_m : melting temperature [°C]
T_{amb} : ambient temperature [°C]
V : velocity [m·s^{-1}]
X, Y : horizontal and vertical coordinates, respectively

Greek Letters

α : absorptivity
β : thermal expansion coefficient of PCM
ε : emissivity coefficient
Ω : solid angle

σ : Stefan-Boltzmann constant=5.67E_8 W/(m^2 K^4)
ΔT : transition temperature [K]
ρ : density [kg/m^3]
λ : latent heat [J kg^{-1}]

DECLARATIONS

The authors declare that they have no known competing financial interests or personal relationships that could have appeared to influence the work reported in this paper.

Ethics Approval

Not applicable.

This article does not contain any studies with human participants or animals performed by any of the authors.

Consent to Participate

Not applicable

Consent for Publication

Not applicable

Availability of Data and Materials

The data will be made available on request

Code Availability

The Code will be made available on Reasonable request

Conflicts of Interest/Competing Interests

The authors declare that they have no conflicts of interest/competing interests

Funding

Not applicable

Manuscript Acknowledgements

Not applicable

CONFLICT OF INTEREST STATEMENT

On behalf of all authors, the corresponding author states that there is no conflict of interest.

DATA AVAILABILITY STATEMENT

The data will be made available on reasonable request.

REFERENCES

1. K. K. W. Wan, D. H. W. Li, D. Liu and J. C. Lam, *Build. Environ.*, **46**(1), 223 (2011).
2. L. F. Cabeza, A. Castell, C. D. Barreneche, A. De Gracia and A. I. Fernández, *Renew. Sust. Energy Rev.*, **15**(3), 1675 (2011).
3. M. Pomianowski, P. Heiselberg and Y. Zhang, *Energy Build.*, **67**, 56 (2013).
4. N. Soares, J. J. Costa, A. R. Gaspar and P. Santos, *Energy Build.*, **59**, 82 (2013).
5. H. Akeiber, P. Nejat, M. Z. A. Majid, M. A. Wahid, F. Jomehzadeh, I. Z. Famileh and S. A. Zaki, *Renew. Sust. Energy Rev.*, **60**, 1470 (2016).
6. Y. Cui, J. Xie, J. Liu and S. Pan, *Procedia Eng.*, **121**, 763 (2015).
7. A. Sarı, *Energy Build.*, **69**, 184 (2014).
8. V. A. A. Raj and R. Velraj, *Renew. Sust. Energy Rev.*, **14**(9), 2819 (2010).
9. C. Barreneche, H. Navarro, S. Serrano, L. F. Cabeza and A. I. Fernández, *Energy Procedia*, **57**, 2408 (2014).
10. J. Giro-Paloma, M. Martínez, L. F. Cabeza and A. I. Fernández, *Renew. Sust. Energy Rev.*, **53**, 1059 (2016).
11. M. Alam, H. Jamil, J. Sanjayan and J. Wilson, *Energy Build.*, **78**, 192 (2014).
12. L. F. Cabeza, C. Castellon, M. Nogues, M. Medrano, R. Leppers and O. Zubillaga, *Energy Build.*, **39**(2), 113 (2007).
13. X. Jin, M. A. Medina and X. Zhang, *Appl. Therm. Eng.*, **103**, 1057 (2016).
14. J. Xie, W. Wang, J. Liu and S. Pan, *Sol. Energy*, **162**, 533 (2018).
15. C. K. Halford and R. F. Boehm, *Energy Build.*, **39**(3), 298 (2007).
16. A. Fateh, D. Borelli, F. Devia and H. Weinläder, *Therm. Sci. Eng. Prog.*, **6**, 361 (2018).
17. A. Baniassadi, B. Sajadi, M. Amidpour and N. Noori, *Sust. Energy Technol. Assess.*, **14**, 92 (2016).\
18. E. M. Alawadhi, *Energy Build.*, **40**(3), 351 (2008).
19. M. A. Izquierdo-Barrientos, J. F. Belmonte, D. Rodríguez-Sánchez, A. E. Molina and J. A. Almendros-Ibáñez, *Appl. Therm. Eng.*, **47**, 73 (2012).
20. Q. Wang, R. Wu, Y. Wu and C. Y. Zhao, *Energy Build.*, **172**, 328 (2018).
21. K. Kant, A. Shukla and A. Sharma, *Sol. Energy*, **155**, 1233 (2017).
22. K. Saafi and N. Daouas, *Energy*, **187**, 115987 (2019).
23. M. Arıcı, F. Bilgin, S. Nižetić and H. Karabay, *Appl. Therm. Eng.*, **165**, 114560 (2020).
24. M. Arıcı, F. Bilgin, M. Krajčík, S. Nižetić and H. Karabay, *Energy*, **252**, 124010 (2022).
25. E. Tunçbilek, M. Arıcı, M. Krajčík, Y. Li, M. Jurčević and S. Nižetić, *Int. J. Energy Res.*, **46**(14), 20249 (2022).
26. S. A. Memon, H. Z. Cui, H. Zhang and F. Xing, *Appl. Energy*, **139**, 43 (2015).
27. K. Biswas, J. Lu, P. Soroushian and S. Shrestha, *Appl. Energy*, **131**, 517 (2014).
28. J. Sage-Lauck and D. Sailor, *Energy Build.*, **79**, 32 (2014).
29. M. Kheradmand, M. Azenha, J. L. de Aguiar and J. Castro-Gomes, *Energy*, **94**, 250 (2016).
30. D. Li, Y. Zheng, C. Liu and G. Wu, *Energy Convers. Manage.*, **100**, 147 (2015).
31. A. Tokuç, T. Başaran and S. C. Yesügey, *Energy Build.*, **102**, 91 (2015).
32. M. Jaworski, P. Łapka and P. Furmański, *Appl. Energy*, **113**, 548 (2014).
33. M. Arıcı, M. Tükel, C. Yıldız, D. Li and H. Karabay, *Energy Build.*, **229**, 110515 (2020).
34. M. F. Modest and S. Mazumder, *Radiative heat transfer*, Academic Press (2021).